Controlled assembly of SERS substrates templated by colloidal crystal films

Daniel M. Kuncicky, Brian G. Prevo and Orlin D. Velev*

DOI: 10.1039/b512734c

Convective assembly at high volume fractions was used to assemble gold nanoparticles into structured porous films templated by colloidal crystals. These gold nanofilms have hierarchical porosity and were proven to be stable and efficient substrates for surface-enhanced Raman spectroscopy (SERS). The control over the film structure allowed optimization of their performance for potential sensor applications.

Colloidal crystals are materials with periodic structure on the submicrometre length scale made by self-assembly of colloidal particles. Colloidal crystals can be used as a basis for fabrication of photonic materials,[1–7] optical coatings and filters,[8–10] lithographic etching masks,[11–13] and sensors.[14–17] The colloidal crystals can also serve as templates for a variety of other self-assembled materials with controlled and reproducible structure. In this review we highlight results based on our process for rapid and reproducible deposition of colloidal crystal films by convective assembly at high volume fractions.[18] These crystal films serve as templates of controlled structure for surface-enhanced Raman spectroscopy substrates.[16,19]

The hallmark of SERS is selectivity, potential for remote sampling through fiber optics, and capability for detection of analytes in aqueous solvents. Despite these advantages the widespread use of SERS-based analytical technology has been slow. Before SERS-based sensors can find broad application in routine chemical analysis new SERS materials must be developed that yield consistently high signals and provide detection generality towards a wide range of chemical and environmental analytes. The major requirements for the SERS substrate materials include controlled nanoscale structure, periodicity and chemical stability. One of the well-studied methods for making SERS substrates uses mono- and bi-layers of close-packed microsphere

Department of Chemical and Biomolecular Engineering, North Carolina State University, Raleigh, NC 27695, USA.
E-mail: odvelev@unity.ncsu.edu

Daniel Kuncicky

Daniel Kuncicky is a PhD candidate in the Department of Chemical and Biomolecular Engineering at North Carolina State University. He received his BS in Chemical Engineering from the University of Florida in 2001. He is working in the field of colloids science with an emphasis on developing new substrates for chemical detection by surface-enhanced Raman scattering.

Brian Prevo

Brian Prevo received his BS in Chemical Engineering from the University of California, Davis in 2001. His graduate research with Velev included convective assembly of nanoparticle coatings and collaborative projects involving ferritin proteins, droplet microfluidics and colloidal assembly from compressed carbon dioxide. His PhD defense is scheduled for November 2005.

Orlin Velev

Orlin Velev leads a research group at NCSU which studies and develops nanostructures with electrical and photonic functionality, biosensors and microfluidic devices. He has been one of the first to synthesize ''inverse opals'', colloidosomes, develop microscopic biosensors and discover novel types of self-assembling microwires. He has contributed more than 70 publications, which have been cited more than 2200 times. For more information see http://crystal.che.ncsu.edu/

crystals as masks.[20] Ordered arrays of separated silver nanoparticles are fabricated by evaporating metal through the microsphere masks. This ''nanosphere lithography'' fabrication technique has yielded important data on the effect of particle size, shape, ordering and surface functionalization on the optical properties and SERS behavior.[21–23] Ordering and periodicity of the metal islands made by ''natural lithography'' or microfabrication have also been shown to improve the substrate SERS performance.[24,25]

A simpler and potentially powerful alternative to vacuum-based metal deposition processes is to make SERS materials by immobilizing SERS-active metal nanoparticles onto a solid support. Colloidal suspensions of gold and silver nanoparticles are often used because they are easily prepared, and yield high Raman enhancement.[26] If the nanoparticles are aggregated, it is thought that intense electric field coupling in ''hot spot'' regions between adjacent nanoparticles can engender higher enhancement.[27,28] An intrinsic advantage of the self-assembled nanoparticle films is their high surface area available for analyte adsorption. The fabrication of such substrates, however, requires the design of wet-assembly techniques that are controllable, precise and reproducible, which has proven to be an overarching problem in most nanoparticle assembly processes. As a consequence, novel techniques for fabricating thin nanoparticle films have garnered much attention. In a well-known example of a nanoparticle deposition method for SERS, biospecific or metal-affinity interactions are exploited to attach metallic nanoparticles to a glass or silicon oxide surface.[29] Alternatively, SERS materials have been made from nanoparticles deposited *via* electrolyte induced aggregation and sedimentation.[30] Deposits of nanoshells,[31] aggregated nanorods,[32] and other anisotropic nanoparticles[33] have high SERS activity as well. In most cases, however, such nanoparticle layers are disordered and lack long-range periodicity.

In our study we used convective assembly to deposit films from chemically unmodified metallic nanoparticles on plain non-functionalized glass substrates. We developed a procedure for nanoparticle concentration by membrane filtration *via* centrifugation, and an apparatus for convective assembly at high volume fractions (Fig. 1) that allows rapid deposition of nanocoatings.[18,34,35] The combination of these two techniques allowed controlled and efficient assembly of a wide variety of thin structures from as-synthesized gold nanoparticles. The data presented here highlight our efforts to engineer the structure of such self-assembled substrates in order to optimize their performance in realistic sensor applications.

Templating metallic nanoparticles into ''inverse opal'' films

The apparatus for convective assembly requires only microlitres of suspension and less than an hour of deposition time without the need for any complex or costly equipment. The particles dispersed in the liquid are transported to the edge of the growing crystal by the flux of the liquid compensating for evaporation from the crystal surface (Fig. 1). This process, referred to as ''convective assembly''[3,36] or ''evaporation induced self-assembly,''[37] takes place near the meniscus of evaporating liquid films. The particles concentrated and confined in the thin film are ordered into a colloidal crystal by reduction of free volume and capillary immersion forces.[38] The mechanism is similar to the popularized ''coffee ring'' effect.[39,40] For thin films of spherical particles, the predominant microstructure formed is hexagonal close-packed crystals with (111) plane oriented parallel to the substrate. These films are typically polycrystalline due to multiple nucleation sites along the drying region. Arrays with square ordering are seen locally, but they appear to be a transition phase between the more stable hexagonally packed regions.[18] In the confined geometry of thin films there is a competition between the thermodynamically favored packing density and the film thickness available to the particle layers. Square arrays are the thermodynamically preferred organization in layers of certain thickness,[41] however it is rarely observed in films deposited only from latex spheres. This is likely due to the flexibility of the liquid–air interface, which permits particle protrusion through the liquid meniscus, hence allowing the formation of the hexagonal, rather than square, arrays.[18]

The method could be adapted for a single step fabrication of templated metallic nanostructures *via* convective assembly of a binary mixture of sacrificial microspheres and metallic nanoparticles (Fig. 1). Small nanoparticles (10–20 nm) added to the suspension

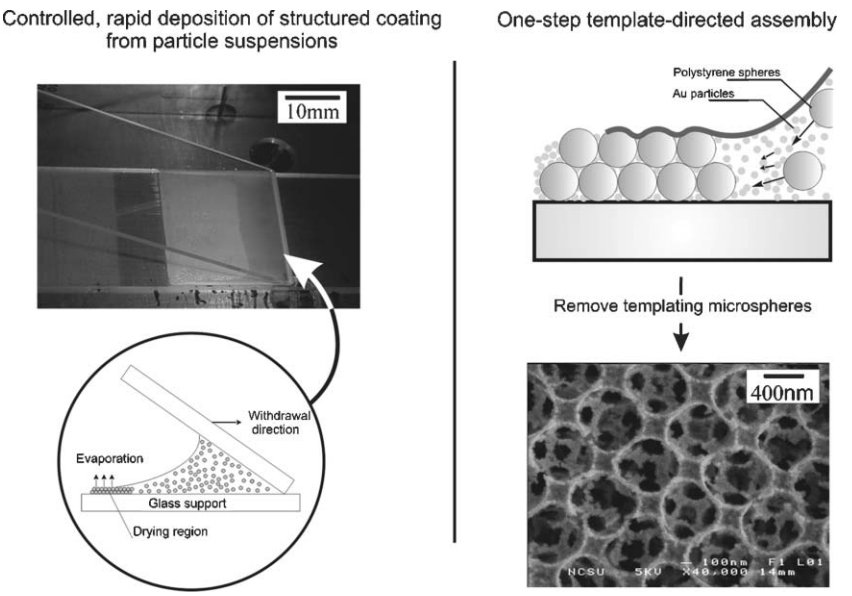

Fig. 1 Schematic of the experimental setup for colloidal crystal assembly (left), and one-step template directed fabrication of SERS substrates (right). The order–disorder transition between the meniscus and the iridescent deposited crystal is clearly visible in the upper left image showing the actual process of deposition of a colloidal crystal coating.

infiltrate the interstitial space surrounding the larger sacrificial microspheres (400–1000 nm). The aggregated nanoparticles replicate the microstructure imparted by the larger aggregated spheres. The templating spheres can be removed after deposition to yield an "inverse opal" metal film of defined thickness (Fig. 1). The presence of the concentrated nanoparticles during the convective assembly process assists the formation of microsphere crystals with square packing symmetry. This type of lattice likely results from the reduced mobility (geometric confinement) of the larger microspheres in drying films of mixed concentrated particles.

Probing the structure-dependent SERS performance of the templated metallic films

The template-directed convective assembly technique allows for tuning the porosity on two hierarchical length scales. Microstructured cavities remain after removing the sacrificial template, and smaller nanopores are formed in between the gold particles. The size of these features can be controlled by varying the size of latex beads and the gold nanoparticles used during assembly. Our structures are comprised of continuously aggregated nanoscopic gold particles arranged into a periodic network of high surface area. They differ from the arrays of discrete submicron silver or gold tetrahedral particles made by top-down nanosphere lithography.[13] Consequently, these different structures allow for different types of SERS experiments and responses, but a direct comparison of the enhancement per unit metal surface is rather difficult.

The type, quality and structure of the template colloidal crystal depend primarily on the withdrawal speed and volume fraction of the colloidal suspensions used in the process.[18,19] By varying these parameters we fabricated latex templates that were polycrystalline with single crystal dimensions in the 5–20 μm range, or randomly packed with no apparent long-range crystal order (Fig. 2). As a control, gold nanoparticle films were also prepared without using latex templating. All experimental measurements were performed using a point sampling protocol in a microfluidic flow cell.[16,19] Such online flow cells could be directly used as a basis for SERS sensors for continuous monitoring of water or gas fluxes. Post-deposition treatment of the nanoparticle layers with dimethyldichlorosilane vapor hydrophobized the glass substrates, enhancing the adhesion of the gold films, and improving their stability to the extent that they can be subjected to prolonged exposure to shear flows in the experimental cells.[16] A matrix of experiments was designed to isolate individual contributions to the Raman enhancement arising from the nano- and microstructure.[19] We collected multiple data points from randomly chosen spots on each SERS substrate inside the microfluidic chamber filled with liquid. This simulates application in real sensors where no drying and alignment to find "hot spots" is usually possible. Statistical analysis of the data was performed to determine the sensitivity of the substrates, and reproducibility of the fabrication technique. The porous gold substrates had a limit of detection of 150 ppb for sodium cyanide in water based on a five percent probability of false alarm.[42] Furthermore, the substrates performed well over a broad range of concentrations and pH values.[16]

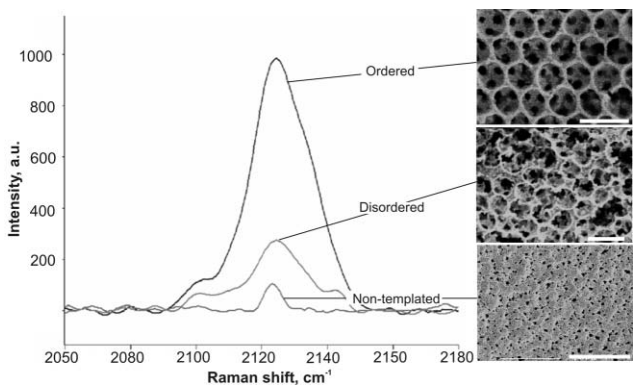

Fig. 2 Effect of substrate structure on the SERS signal intensity. Characteristic sodium cyanide spectra and SEM images collected in the continuous sampling microfluidic flow cell for ordered latex-templated (top), disordered latex-templated (middle), and non-templated (bottom) SERS substrates. Scale bars are 1 μm (top and middle micrographs) and 10 μm (bottom micrograph).[19]

The most intense SERS signals were reproducibly obtained on films with ordered polycrystalline micropores similar to the ones shown in Fig. 2. We observed a multifold increase in intensity of the 2125 cm^{-1} peak for cyanide adsorbed on the ordered crystalline regions compared with the disordered regions. The substrates without any templating were weakly enhancing, with a signal up to an order of magnitude lower than the microsphere templated ones. The variability of the peak intensity for the templated substrates (both ordered and disordered) was *ca.* 20% compared with *ca.* 75% for the non-templated variety.[42] One of the major reasons SERS is not a widely used technology is the lack of standardized substrates that have uniform and reproducible SERS performance on any equipment. Poor reproducibility and hence high false alarm rates can be a fatal flaw for any routine diagnostic technique. These results demonstrate that the engineered templated deposition could produce substrates with consistently high signals, and may be an effective route to make substrates for SERS-based sensors for practical chemical analysis.

The convective assembly method also allows characterization of the effect of substrate thickness by depositing films with controlled numbers of nanoparticle layers. These experiments, however, were performed with non-templated films, as the structure of the colloidal crystals varies with the number of layers.[18] We found that the nanoparticle film thickness has little effect on SERS signal intensity for substrates thicker than a monolayer. This finding probably reflects the fact that only the particles in the top layer are illuminated by the excitation laser and hence contribute to the SERS signal. The practical significance is that only a relatively thin layer of gold nanoparticles is required to generate a strong signal.

Finally we characterized the effect of the nanoporosity inherent in the

aggregated structure of adjacent nanoparticles. The nanoporosity can be changed by controlled post-deposition fusion of the gold nanoparticles at temperatures between 200 and 500 °C.[43] In order to reliably characterize the effect of the nanoporosity on SERS performance we developed a procedure for making nanoporosity gradient substrates by imposing a monotonically varying thermal gradient onto the backside of the SERS support.[19] This technique produced substrates that had fully fused gold nanoparticles on one end and unchanged discrete aggregated gold nanoparticles on the other, with a variable degree of fusion in the middle. The degree of nanoporosity along the sample surface after heating could be correlated to the spatially varying color change. The substrate retained its characteristic reddish brown color on the non-fused side and gradually took on a golden color towards the fully fused end. The formation of large continuous metal domains from fused particles was evidenced by the extreme broadening of the surface plasmon resonance (SPR) adsorption peak centered on 780 nm. Examination of the heat-treated end of substrates with SEM verified that the microscale pores left over from latex templates were retained throughout the entire film structure.

The SERS signal was highest for the unheated region, and decreased commensurate with the degree of particle fusing (Fig. 3). These data convincingly demonstrate that nanoscale surface roughness stemming from the discrete aggregated gold particles is a key factor directly related to high SERS performance. While it may be expected that nanoscale roughness generates stronger plasmon resonances, this may not be the only major effect here. Our working hypothesis is that the strong SERS response collected from the nanoporous substrates is closely related to the large surface area which allows more analyte to adsorb from the surrounding solution.

Concluding remarks

The cycle of experiments discussed here proved that while both the micro- and the nanostructure contribute to the high enhancement of our substrates it is the nanopores that lead to the key effect. The presence of sub-micron pores left behind by the sacrificial latex beads and the long-range ordering of these large pores also contribute to the enhancement of these substrates. These SERS substrates are simple and inexpensive to prepare: less than a milligram of nanoparticles is required to coat a surface of tens of square millimetres. The gold substrates were proven to be highly stable and to have a shelf life of at least a year. Since they are made from inert gold, the problem of physical and chemical deterioration common to silver-based SERS substrates is avoided.

The metallic substrates fabricated to date by us and by others suffer from a major drawback; they rely on the binding of the agent being analyzed to the surface of the nanoparticle arrays, or its deposition in a dry state on top of the substrates. The strong binding of the CN^- ions to the gold and silver substrates appears to be the major factor behind the easy detection of cyanides, while the weak adsorption of non-polar molecules makes detection difficult. This problem is avoided in widely used protocols where chemical agent samples are dried on top of substrates dipped in the solution. Drying concentrates the sample and physically forces solids into the regions with SERS activity. This method, however, can introduce data artifacts, will not work with volatile analytes and can not be used in on-line continuous sampling. For this reason, we are presently focused on experiments in microfluidic continuous-flow chambers such as the ones discussed above. A major direction for future research in the area will be the chemical functionalization of our substrates with the aim of targeting specific analytes.

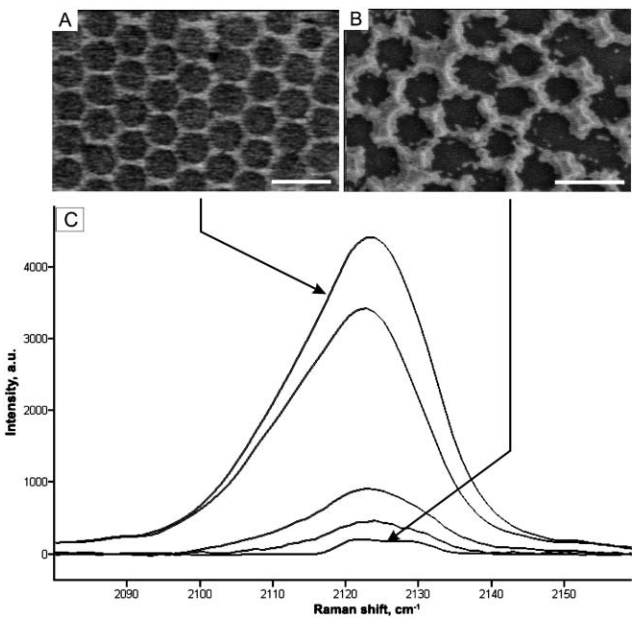

Fig. 3 Effect of the substrate nanoporosity on SERS spectra intensity. SEM images collected from the (A) non-fused and (B) fused regions of the substrate with a nanoporosity gradient. Scale bars = 1 μm. (C) Raman spectra collected sequentially moving from the non-fused end (top spectra) to the highly-fused end (bottom spectra).[19]

Acknowledgements

We are thankful to Steven Christesen for insightful discussions. This research was supported by grants from the US Army Research Office and National Institutes of Health.

References

1 A. van Blaaderen, R. Ruel and P. Wiltzius, *Nature*, 1997, **385**, 321.
2 O. D. Velev, T. A. Jede, R. F. Lobo and A. M. Lenhoff, *Nature*, 1997, **389**, 447.
3 P. Jiang, J. F. Bertone, K. S. Hwang and V. L. Colvin, *Chem. Mater.*, 1999, **11**, 2132.
4 Y. A. Vlasov, X. Z. Bo, J. C. Sturm and D. J. Norris, *Nature*, 2001, **414**, 289.
5 O. D. Velev and E. W. Kaler, *Adv. Mater.*, 2000, **12**, 531.
6 W. Lee, A. Chan, M. A. Bevan, J. A. Lewis and P. V. Braun, *Langmuir*, 2004, **20**, 5262.

7 Y. Lin, P. R. Herman, C. E. Valdivia, J. Li, V. Kitaev and G. A. Ozin, *Appl. Phys. Lett.*, 2005, **86**, 121106.
8 S. H. Park and Y. N. Xia, *Langmuir*, 1999, **15**, 266.
9 P. Mach, P. Wiltzius, M. Megens, D. A. Weitz, K. H. Lin, T. C. Lubensky and A. G. Yodh, *Europhys. Lett.*, 2002, **58**, 679.
10 B. G. Prevo, Y. Hwang and O. D. Velev, *Chem. Mater.*, 2005, **17**, 3642.
11 D. G. Choi, H. K. Yu, S. G. Jang and S. M. Yang, *J. Am. Chem. Soc.*, 2004, **126**, 7019.
12 N. H. Finkel, B. G. Prevo, O. D. Velev and L. He, *Anal. Chem.*, 2005, **77**, 1088.
13 A. J. Haes, C. L. Haynes, A. D. McFarland, G. C. Schatz, R. R. Van Duyne and S. L. Zou, *MRS Bull.*, 2005, **30**, 368.
14 J. H. Holtz and S. A. Asher, *Nature*, 1997, **389**, 829.
15 J. Zhou, C. Q. Sun, K. Pita, Y. L. Lam, Y. Zhou, S. L. Ng, C. H. Kam, L. T. Li and Z. L. Gui, *Appl. Phys. Lett.*, 2001, **78**, 661.
16 P. M. Tessier, S. D. Christesen, K. K. Ong, E. M. Clemente, A. M. Lenhoff, E. W. Kaler and O. D. Velev, *Appl. Spectrosc.*, 2002, **56**, 1524.
17 Y. J. Lee, S. A. Pruzinsky and P. V. Braun, *Langmuir*, 2004, **20**, 3096.
18 B. G. Prevo and O. D. Velev, *Langmuir*, 2004, **20**, 2099.
19 D. M. Kuncicky, S. D. Christesen and O. D. Velev, *Appl. Spectrosc.*, 2005, **59**, 401.
20 J. C. Hulteen and R. P. Van Duyne, *J. Vac. Sci. Technol., A*, 1995, **13**, 1553.
21 T. R. Jensen, M. D. Malinsky, C. L. Haynes and R. P. Van Duyne, *J. Phys. Chem. B*, 2000, **104**, 10549.
22 T. Vo-Dinh, *TrAC, Trends Anal. Chem.*, 1998, **17**, 557.
23 K. E. Shafer-Peltier, C. L. Haynes, M. R. Glucksberg and R. P. Van Duyne, *J. Am. Chem. Soc.*, 2003, **125**, 588.
24 R. L. Moody, T. Vo-Dinh and W. H. Fletcher, *Appl. Spectrosc.*, 1987, **41**, 966.
25 M. Kahl, E. Voges, S. Kostrewa, C. Viets and W. Hill, *Sens. Actuators, B*, 1998, **51**, 285.
26 M. Kerker, D. S. Wang and H. Chew, *Appl. Opt.*, 1980, **19**, 4159.
27 V. M. Shalaev, R. Botet, J. Mercer and E. B. Stechel, *Phys. Rev. B*, 1996, **54**, 8235.
28 A. M. Michaels, J. Jiang and L. Brus, *J. Phys. Chem. B*, 2000, **104**, 11965.
29 R. G. Freeman, K. C. Grabar, K. J. Allison, R. M. Bright, J. A. Davis, A. P. Guthrie, M. B. Hommer, M. A. Jackson, P. C. Smith, D. G. Walter and M. J. Natan, *Science*, 1995, **267**, 1629.
30 M. Suzuki, Y. Niidome, Y. Kuwahara, N. Terasaki, K. Inoue and S. Yamada, *J. Phys. Chem. B*, 2004, **108**, 11660.
31 J. B. Jackson and N. J. Halas, *Proc. Natl. Acad. Sci. USA*, 2004, **101**, 17930.
32 S. Link, D. J. Hathcock, B. Nikoobakht and M. A. El-Sayed, *Adv. Mater.*, 2003, **15**, 393.
33 Z. Q. Tian, B. Ren and D. Y. Wu, *J. Phys. Chem. B*, 2002, **106**, 9463.
34 P. M. Tessier, O. D. Velev, A. T. Kalambur, J. F. Rabolt, A. M. Lenhoff and E. W. Kaler, *J. Am. Chem. Soc.*, 2000, **122**, 9554.
35 P. M. Tessier, O. D. Velev, A. T. Kalambur, A. M. Lenhoff, J. F. Rabolt and E. W. Kaler, *Adv. Mater.*, 2001, **13**, 396.
36 N. D. Denkov, O. D. Velev, P. A. Kralchevsky, I. B. Ivanov, H. Yoshimura and K. Nagayama, *Langmuir*, 1992, **8**, 3183.
37 C. J. Brinker, Y. F. Lu, A. Sellinger and H. Y. Fan, *Adv. Mater.*, 1999, **11**, 579.
38 P. A. Kralchevsky and N. D. Denkov, *Curr. Opin. Colloid Interface Sci.*, 2001, **6**, 383.
39 R. D. Deegan, O. Bakajin, T. F. Dupont, G. Huber, S. R. Nagel and T. A. Witten, *Nature*, 1997, **389**, 827.
40 H. Hu and R. G. Larson, *J. Phys. Chem. B*, 2002, **106**, 1334.
41 B. Pansu, P. Pieranski and L. Strzelecki, *J. Phys. (Paris)*, 1983, **44**, 531.
42 D. M. Kuncicky, S. D. Christesen and O. D. Velev, *Proc. SPIE-Int. Soc. Opt. Eng.*, 2004, **5585**, 33.
43 B. G. Prevo, J. C. Fuller and O. D. Velev, *Chem. Mater.*, 2005, **17**, 28.